Plasmons enhance near-field radiative heat transfer for graphene-covered dielectrics

V. B. Svetovoy,[1,2] P. J. van Zwol,[3] and J. Chevrier[3]

[1]*MESA+ Institute for Nanotechnology, University of Twente, PO 217, 7500 AE Enschede, The Netherlands*
[2]*Institute of Physics and Technology, Yaroslavl Branch, Russian Academy of Sciences, 150007, Yaroslavl, Russia*
[3]*Institut Néel, CNRS and Université Joseph Fourier Grenoble, Boîte Postale 166, FR-38042 Grenoble Cedex 9, France*

(Dated: January 10, 2012)

It is shown that a graphene layer on top of a dielectric slab can dramatically influence the ability of this dielectric for radiative heat exchange. Effect of graphene is related to thermally excited plasmons. Frequency of these resonances lies in the terahertz region and can be tuned by varying the Fermi level through doping or gating. Heat transfer between two dielectrics covered with graphene can be larger than that between best known materials and even much larger at low temperatures. Moreover, high heat transfer can be significantly modulated by electrical means that opens up new possibilities for very fast manipulations with the heat flux.

PACS numbers: 44.40.+a, 42.50.Lc, 78.67.-n

Radiative heat transfer (RHT) in vacuum at small distances between bodies is much increased in the near-field regime as compared to that given by the black body law [1–3]. It happens due to interaction of evanescent waves at distances small in comparison with the thermal wavelength $\lambda_T = \hbar c/T$ (here $k_B = 1$). Particularly strong enhancement occurs when bodies can support surface modes such as plasmon-polaritons and phonon-polaritons [4, 5]. This effect can be used to improve performance of near-field photovoltaic devices [6], in nanofabrication [7], and in near-field imaging systems [8].

Graphene attracted recently enormous attention as a two dimensional carbon material with unusual electronic properties [9]. It is considered as a promising material for the development of high-performance electronic devices [10, 11]. Plasmons in graphene show favorable behavior for applications such as large confinement, long propagating distances, and high tunability via electrostatic gating [12]. In contrast with nobel-metals the plasmon frequencies lie in the terahertz region that is interesting for radiative heat transfer, but the topic was not explored yet. Heat transfer was considered [13] only between closely spaced graphene and SiO_2 substrate where plasmons do not play significant role.

Pristine graphene at zero temperature does not support plasmon excitations but doped material does [14]. On the other hand at finite temperature plasmons exist even for undoped material [15]. These thermoplasmons were shown to change significantly the thermal Casimir force for suspended graphene [16] and graphene-covered materials [17]. In this paper we show that plasmon excitations in graphene have striking effect on the near-field RHT between bodies if at least one of them is covered with graphene.

Usual local materials have fixed frequencies of phonon-polariton or plasmon-polariton resonances. Graphene is essentially nonlocal material and its plasmon frequency changes with the wavenumber. Moreover, it varies significantly with the doping level. These properties make plasmons in graphene a convenient tool to control the heat transfer between bodies.

To evaluate the RHT between two bodies 1 and 2 one has to know the reflection coefficients r_1^μ and r_2^μ for each body as functions of the frequency ω and the wave vector $\mathbf{q}$. These coefficients are different for each polarization $\mu = s$ (transverse electric) or $\mu = p$ (transverse magnetic). If the separation d between two parallel plates is small in comparison with the thermal wavelength, $d \ll \lambda_T$, only evanescent waves will contribute to the heat transfer. Defining the heat transfer coefficient (HTC) as $h = \Phi(T, T-\Delta T)/\Delta T$ for $\Delta T \to 0$, where $\Phi(T_1, T_2)$ is the heat flux and $\Delta T = T_1 - T_2$ is the temperature difference between bodies, one finds $h = h_p + h_s$, where

$$h_\mu = \frac{1}{4\pi^2 d^2}\int\limits_0^\infty \mathrm{d}\omega \frac{(\hbar\omega/T)^2\, e^{\hbar\omega/T}}{\left(e^{\hbar\omega/T}-1\right)^2}\int\limits_0^\infty \mathrm{d}x \frac{x e^{-x}\,\mathrm{Im}r_1^\mu \mathrm{Im}r_2^\mu}{\left|1-r_1^\mu r_2^\mu e^{-x}\right|^2}. \tag{1}$$

Here the integration variable in the physical terms is $x = 2d\sqrt{q^2-\omega^2/c^2}$.

Suppose that the body i is a dielectric substrate with the dielectric function $\varepsilon_i(\omega)$ covered with a layer of graphene. Reflection coefficient for this body can be found describing graphene as a sheet with a current. Then for p-polarization one has [18]:

$$r_i = \frac{k_0\varepsilon_i - k_i + (4\pi\sigma/\omega)\,k_0 k_i}{k_0\varepsilon_i + k_i + (4\pi\sigma/\omega)\,k_0 k_i}, \tag{2}$$

where $k_0 = \sqrt{\omega^2/c^2 - q^2}$ and $k_i = \sqrt{\varepsilon_i\omega^2/c^2 - q^2}$ are the normal components of the wave vectors in vacuum and in the substrate, respectively, and $\sigma(q,\omega)$ is the two-dimensional (2D) dynamical conductivity of graphene. We omitted the polarization index in (2) because the contribution of graphene can be found using only p-polarization. Moreover, similar to the situation with the Casimir force [16, 17] (see also [19]) we can use the non-retarded approximation to calculate the effect

of graphene. Retardation and the contribution of s-polarization both are suppressed at least by the factor $v_F/c \approx 1/300$, where v_F is the Fermi velocity in graphene. However, it has to be stressed that the non-retarded limit can be applied only to the graphene contribution [17]. For the HTC this contribution is defined as

$$\Delta h = h_p(r_1, r_2) - h_p(r_{10}, r_{20}), \tag{3}$$

where h_p must be understood as a functional defined by Eq. (1) and r_{i0} is the reflection coefficient of the body i without graphene. To calculate any term $h(r_1, r_2)$ or $h(r_{10}, r_{20})$ separately one has to include both the polarization and retardation effects.

Dielectric function of graphene on the interface of vacuum and body i can be calculated in the random phase approximation [9] as $\varepsilon(q,\omega) = 1 + v_c(q)\Pi(q,\omega)$, where $v_c = 2\pi e^2/\kappa_i q$ is the 2D Coulomb interaction, κ_i is defined by the environment of the graphene layer, $2\kappa_i = \varepsilon_i(0)+1$, and $\Pi(q,\omega)$ is the 2D polarizability given by the bare bubble diagram. The latter was calculated in many papers [14, 20]; here we are using the result [17] that can be applied for both finite temperature and finite Fermi level. One can equally express the result via 2D susceptibility $\chi(q,\omega) = (e^2/q^2)\Pi(q,\omega)$, which, in turn, is expressed via 2D conductivity as $-i\omega\chi(q,\omega) = \sigma(q,\omega)$. In this way the reflection coefficient r_i in the non-retarded limit ($c \to \infty$) can be expressed via the dielectric functions of the substrate $\varepsilon_i(\omega)$ and graphene $\varepsilon(q,\omega)$:

$$r_i = \frac{\varepsilon_i - 1 + 2\kappa_i(\varepsilon - 1)}{\varepsilon_i + 1 + 2\kappa_i(\varepsilon - 1)}, \quad c \to \infty. \tag{4}$$

Random phase approximation describes collisionless electron gas, but this approximation is not sufficient for the RHT. This is because the graphene contribution given by Eqs. (3) and (1) disappears in the limit $\mathrm{Im}\varepsilon \to 0$ and finite dissipation is of principal importance. At low frequencies the main dissipation in graphene is due to impurities and defects for electrons [12]. It can be included via the finite relaxation time $\tau \equiv \gamma^{-1}$ as proposed by Mermin [21], where $\gamma = 10^{12} - 10^{13}$ rad/s. In this approach the dielectric function $\varepsilon_\tau(q,\omega)$ is expressed via the collisionless function $\varepsilon(q,\omega)$ taken at complex frequency $\omega \to \omega + i\gamma$ as

$$\varepsilon_\tau(q,\omega) = 1 + \frac{(\omega + i\gamma)\left[\varepsilon(q,\omega+i\gamma) - 1\right]}{\omega + i\gamma\frac{\varepsilon(q,\omega+i\gamma)-1}{\varepsilon(q,0)-1}}. \tag{5}$$

Function ε_τ has to be used in Eq. (4) instead of ε.

At finite doping and finite temperature the function $\varepsilon(q,\omega)$ can be presented in an analytic form in the limit $Q = \hbar v_F q/2T \ll 1$ [17]. In this limit the intraband transitions dominate in the dielectric function, while the interband transitions are suppressed by the factor Q and the dielectric function is

$$\varepsilon(q,\omega) = 1 + \frac{2\alpha_g G(\epsilon_F)}{Q}\left(1 - \frac{\omega}{\sqrt{\omega^2 - v_F^2 q^2}}\right), \tag{6}$$

where $\epsilon_F = E_F/T$ is the dimensionless Fermi level and $\alpha_g = e^2/\kappa\hbar v_F$ is the coupling constant in graphene. Function $G(\epsilon_F)$ is defined as:

$$G(\epsilon_F) = \int_0^\infty \mathrm{d}t t \frac{1 + \cosh t \cosh\epsilon_F}{\left(\cosh t + \cosh\epsilon_F\right)^2}. \tag{7}$$

For small and large values of ϵ_F it takes the asymptotic values $G(\epsilon_F \to 0) = 2\ln 2$ and $G(\epsilon_F \to \infty) = \epsilon_F$, respectively.

Let us assume first that the substrate of the body 1 has no optical activity in the terahertz range. It means that $\varepsilon_1(\omega) \approx \varepsilon_1(0)$. In this case the reflection coefficient has a pole when $\varepsilon(q,\omega) = 0$ ($\gamma \to 0$). This pole describes plasmon in graphene with the dispersion relation

$$\hbar\omega_p(q) \approx \sqrt{2\alpha_g G(\epsilon_F)\hbar v_F q T}, \quad Q \ll 1. \tag{8}$$

When $\epsilon_F \to 0$ we reproduce Vafek's thermoplasmon [15]. In the limit of large ϵ_F the plasmon frequency does not depend anymore on T and we find the plasmon that emerging at finite doping [14].

For the best heat transfer the resonances in the opposing bodies have to match each other [4]. When one body is covered with graphene one can always find a value of the wavenumber q that gives the plasmon resonance matching the resonance in the opposing body.This simple principle gives qualitative explanations for rich physics that can be realized between bodies covered with graphene. Let us illustrate this statement.

Suppose that the second body can be described at low frequencies by a single Lorentz-Drude oscillator with the dielectric function

$$\varepsilon_2(\omega) = \varepsilon_\infty\left(1 + \frac{A\omega_r^2}{\omega_r^2 - \omega^2 - i\Gamma\omega}\right), \tag{9}$$

where ω_r is the resonance frequency, $\Gamma \ll \omega_r$ is the resonance width, A is the amplitude, and ε_∞ is the high-frequency dielectric constant. Reflection coefficient r_2 has the resonance at frequency corresponding to the surface wave excitation that is determined by the equation $\varepsilon_2(\omega) = -1$. This frequency is

$$\omega_{2s} = \omega_r\sqrt{B}, \quad B = \frac{\varepsilon_2(0) + 1}{\varepsilon_\infty + 1}. \tag{10}$$

Imaginary part of r_2 is shown in Fig. 1(a) by the dashed line. Plasmon resonances in graphene give peaks in $\mathrm{Im}r_1$ that are shown for $x = 1$ and $x = 3$. Because $x = 2dq$ there is a value of q when frequencies of the resonances in both bodies match each other.

Integration over x in Eq. (1) gives the spectral density of the HTC shown in Fig. 1(b) for two values of the Lorentz resonance. This density is concentrated around the resonance in the body 2. Integrating over ω one finds the effect of graphene in the HTC. In the rest of the paper we present the results for the scaled HTC defined as

$$\Delta R = (d/100\ \mathrm{nm})^2 \cdot \Delta h. \tag{11}$$

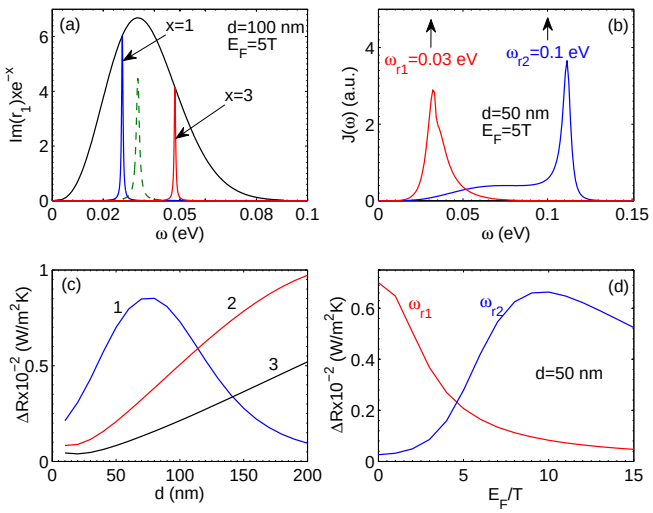

FIG. 1: (Color online) Inactive dielectric covered with graphene (body 1) against a dielectric without graphene described by the Lorentz model (body 2). (a) Resonances in the reflection coefficients. The dashed line (green) shows the fixed resonance in $\mathrm{Im}r_2$. Plasmon resonances in the body 1 are shown for $x = 1$ and $x = 3$ together with the enveloping line (black). (b) Spectral density for two values of the Lorentz resonance. (c) ΔR as a function of distance. Curves 1, 2, 3 correspond to ϵ_F =0, 5, 10, respectively. (d) ΔR as a function of the Fermi level.

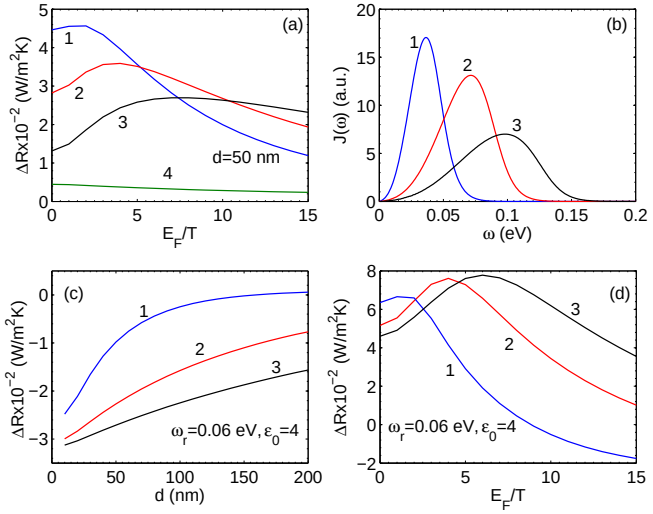

FIG. 2: (Color online) (a) ΔR as a function of ϵ_F for inactive dielectrics both covered with graphene. Curves 1, 2, 3 are for ε_0 =4, 7, 12. Curve 4 is for $\varepsilon_1(0) = 4$ and $\varepsilon_2(0) = 7$. (b) Spectral density for $\varepsilon_0 = 4$ and ϵ_F =0(1), 5(2), 10(3). (c) Two identical substrates described with the Lorentz model; one is covered with graphene; ϵ_F =0(1), 5(2), 10(3). (d) Substrates are the same as in (c) but both covered with graphene. Dependence on ϵ_F is shown for $d = 50(1)$, 100(2), 150(3) nm.

In Fig. 1(c) ΔR is shown for the Lorentz resonance $\omega_{r1} = 0.03$ eV and three different values of the Fermi level. We can compare $h = \Delta R \cdot (100\ \mathrm{nm}/d)^2$ with the black body coefficient $h_{bb} \approx 6\ \mathrm{W/m^2K}$. One can see that graphene provides a significant contribution to the HTC. Dependence of ΔR on the Fermi level is nontrivial and strong. It is shown in Fig. 1(d). Value of ΔR varies more than 10 times when the Fermi level changes from 0 to $10T$. Moreover, this dependence changes from decreasing to increasing when ω_r changes from 0.03 eV to 0.1 eV. Indeed, the characteristic plasmon frequency ω_p^{ch} is given by Eq. (8) for $q \sim 1/2d$. If $\omega_p^{ch} > \omega_r$ for all E_F then ΔR will decrease when the Fermi level increases. In the opposite case ΔR will increase with E_F while the condition $\omega_p^{ch} < \omega_r$ holds true and change to decreasing when the condition is broken.

Effect of graphene is especially strong for identical inactive bodies covered with graphene (see Fig. 2(a)). This is because the plasmons frequencies in both bodies coincide for every q so that the spectral density becomes much wider than in the case of one graphene-covered body. This density is shown in Fig. 2(b) for different values of E_F. The amplitude and width of the curves is essentially controlled by the thermal factor in Eq. (1). Value of ΔR becomes smaller when the substrate dielectric constant $\varepsilon_1(0) = \varepsilon_2(0) = \varepsilon_0$ increases. It is also reduced very fast when the substrates are not the same. This is because the plasmon frequencies do not match any more due to different coupling constants α_g in the graphene layers of different bodies. When one or both of the substrates are metals the effect of graphene disappears, $\Delta R \to 0$. It happens because in the limit $\varepsilon_i \to \infty$ the reflection coefficients with and without graphene coincide, $r_i \to r_{i0}$.

Suppose that body 1 is covered with graphene but both substrates are optically active and can be presented by the same Lorentz oscillator. In this case the body 1 supports two surface waves with the frequencies

$$2(\omega_{1s}^2)_{1,2} = \omega_{2s}^2 + B\omega_p^2 \pm \sqrt{(\omega_{2s}^2 + B\omega_p^2)^2 - 4\omega_{2s}^2\omega_p^2}. \quad (12)$$

These frequencies do not coincide with ω_{2s}. Only in the limit $\omega_p \to 0$ one has $(\omega_{1s})_1 \to \omega_{2s}$. It means that the resonances in different bodies never match each other and the term $h_p(r_1, r_2)$ in Eq. (3) cannot be large. On the other hand, the term $h_p(r_{10}, r_{20})$ must be large because without graphene on body 1 the resonances coincide. Therefore, for identical optically active substrates, graphene on one of the bodies will reduce the heat transfer, $\Delta R < 0$, as demonstrated in Fig. 2(c). Indeed, the total HTC given by Eq. (1) is always positive.

When both active substrates are covered with graphene then the resonances in different bodies match and the spectral density is wide similar to that shown in Fig. 2(b). Difference with the case of inactive substrates is that the term $h_p(r_{10}, r_{20})$ in Eq. (3) is nonzero and gives important negative contribution. Now ΔR can be negative or positive depending on the parameters as shown in Fig. 2(d).

For applications in nanoelectronics it is interesting to have a device that can open and close a heat transfer channel at high switching rate [22]. Bodies covered with graphene allow deep modulation of the heat flux at very

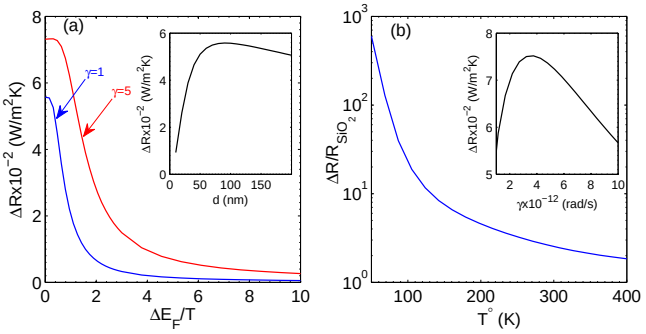

FIG. 3: (Color online) (a) ΔR between two inactive dielectrics ($\varepsilon_0 = 3$) covered with graphene as a function of the Fermi level difference $\Delta E_F = E_{F1} - E_{F2}$; γ is in units 10^{12} rad/s. The inset shows how the maximal value depends of the distance d. (b) Ratio of the HTC for graphene-covered dielectrics (ΔR) and two SiO_2 plates (R_{SiO_2}).The inset presents dependence of the maximal ΔR on the relaxation frequency.

high frequencies. The switching frequency f must be smaller than important frequencies in the graphene dielectric functions, $f \ll v_F/4\pi d \sim 1$ THz but actual restriction comes from graphene electronics that can be switched at frequencies up to 100 GHz [23]. The largest heat flux one can get for identical substrates inactive in THz range that have low dielectric constant in this range. Many polymeric materials used in electronics [24] meet these conditions, for example, polyimide.

When graphene layers on both substrates are equally doped, then the HTC is large but does not change much with the Fermi level as shown in Fig. 2(a). However, when the doping in each layer is different the HTC decreases rapidly because of mismatch of the plasmon frequencies in the graphene layers. Due to this dependence one can modulate the heat transfer between bodies by changing the difference between the Fermi levels in different bodies. Situation is illustrated in Fig. 3(a). HTC decreases 30 times or more when ΔE_F changes from zero to $10T$. The latter value is realized for a reasonable difference in the carrier density around $\Delta n = 5 \cdot 10^{12}$ cm^{-2} at $T = 300°$ K. Maximal value of ΔR varies to some degree with the relaxation frequency γ in graphene as shown in the right inset and with the distance d as shown in the left inset. It has to be stressed that ΔR between identical inactive dielectrics covered with graphene is larger than that between two SiO_2 plates. Note that SiO_2 is considered as one of the very best material for the radiative heat transfer, for which $R_{SiO_2} = 296$ W/m^{2}K at $T = 300°$ K. With temperature decrease R_{SiO_2} decreases fast due to the thermal factor in (1), but ΔR decreases much slower because of plasmon tuning. As the result the ratio $\Delta R/R_{SiO_2}$ increases significantly with T decrease as shown in Fig. 3(b).

In conclusion, we analyzed the change in the near-field radiative heat transfer for materials covered with graphene. Plasmon excitations in graphene change drastically material's ability to the heat transfer. Plasmon frequency is tunable and depends on the wavenumber, Fermi level, temperature, and the substrate dielectric constant. Plasmons can be tuned with the resonances in the opposite body to maximize the HTC. The strongest effect is reached for terahertz-inactive dielectrics with low dielectric constant covered with graphene. In this case the HTC is larger than for the best known materials especially at low temperatures. HTC can be reduced 100 times or so by changing the relative carrier concentration in different bodies. This opens up the possibility to control the heat flux at frequencies as high as 100 GHz.

[1] D. Polder and M. Van Hove, Phys. Rev. B **4**, 3303 (1971).
[2] J.-P. Mulet, K. Joulain, R. Carminati, and J.-J. Greffet, Appl. Phys. Lett. **78**, 2931 (2001).
[3] A. Kittel, W. Müller-Hirsch, J. Parisi, S. A. Biehs, D. Reddig, M. Holthaus, Phys. Rev. Lett. **95**, 224301 (2005).
[4] K. Joulain, J.-P. Mulet, F. Marquier, R. Carminati, and J.-J. Greffet, Surf. Sci. Rep. **57**, 59 (2005); A. I. Volokitin and B. N. J. Persson, Rev. Mod. Phys. **79**, 1291 (2007).
[5] S. Shen, A. Narayanaswamy, and G. Chen, Nano Lett. **9**, 2909 (2009); E. Rousseau, A. Siria, G. Jourdan, S. Volz, F. Comin, J. Chevrier, and J.-J. Greffet, Nat. Photonics **3**, 514 (2009).
[6] M. Laroche, R. Carminati, and J.-J. Greffet, J. Appl. Phys. **100**, 063704 (2006); K. Park, S. Basu, W. P. King, and Z. M. Zhang, JQSRT **109**, 305 (2008).
[7] Z. W. Liu, Q. H. Wei, and X. Zhang, Nano Lett. **5**, 957 (2005); L. Wang, S. M. Uppuluri, E. X. Jin, and X. F. Xu, Nano Lett. **6**, 361 (2006); B. J. Lee, Y. B. Chen, and Z. M. Zhang, JQSRT **109**, 608 (2008).
[8] Y. De Wilde *et al.*, Nature **444**, 740 (2006).
[9] A. H. Castro Neto, F. Guinea, N. M. R. Peres, K. S. Novoselov, and A. K. Geim, Rev. Mod. Phys. **81**, 109 (2009).
[10] K. I. Boloting *et al.*, Solid State Commun. **146**, 351 (2008).
[11] Y.-M. Lin *et al.*, Science **332**, 1294 (2011).
[12] M. Jablan, H. Buljan,and M. Soljačić, Phys. Rev. B **80**, 245435 (2009); F. H. Koppens, D. E. Chang, and F. J. G. de Abajo, arXiv: 1104.2068; L. Ju *et al.*, Nat. Nanotechnol **6**, 630 (2011);
[13] B. N. J. Persson and H. Ueba, J. Phys.: Condens. Matter **22**, 462201 (2010); A. I. Volokitin and B. N. J. Persson, Phys. Rev. B **83**, 241407(R) (2011).
[14] B. Wunsch, T. Stauber, and F. Guinea, New. J. Phys. **8**, 318 (2006); E. H. Hwang and S. Das Sarma, Phys. Rev. B **75**, 205418 (2007).
[15] O. Vafek, Phys. Rev. Lett. **97**, 266406 (2006).
[16] G. Gómez-Santos, Phys. Rev. B **80**, 245424 (2009).
[17] V.B. Svetovoy, Z. Moktadir, M. C. Elwenspoek, and H. Mizuta, EPL **96**, 14006 (2011).
[18] L. A. Falkovsky and S. S. Pershoguba, Phys. Rev. B **76**, 153410 (2007); T. Stauber, N. M. R. Peres, and A. K. Geim, Phys. Rev. B **78**, 085432 (2008).
[19] I. V. Fialkovsky, V. N. Marachevsky, and D. V. Vassile-

vich, Phys. Rev. B **84**, 035446 (2011).
[20] V. N. Kotov, B. Uchoa, V. M. Pereira, A. H. Castro Neto, and F. Guinea, arXiv:1012.3484.
[21] N. D. Mermin, Phys. Rev. B **1**, 2362 (1970).
[22] P. J. van Zwol, K. Joulain, P. Ben Abdallah, J. J. Greffet and J. Chevrier, Phys. Rev. B **83**, 201404(R) (2011).
[23] Y.-M. Lin *et al.*, Science **327**, 662 (2010); Y. Wu *et al.*, Nature **472**, 74 (2011).
[24] X.-Y. Zhao and H.-J. Liu, Polym. Int. **59**, 597 (2010).